Available online at www.sciencedirect.com
SCIENCE DIRECT®
Journal of Molecular Spectroscopy 217 (2003) 195–211
Journal of MOLECULAR SPECTROSCOPY
www.elsevier.com/locate/jms

(0 0 0) and (0 1 0) States of $H_2{}^{18}O$: analysis of rotational transitions in hot emission spectrum in the 400–850 cm^{-1} region

S.N. Mikhailenko,[a] Vl.G. Tyuterev,[b,*] and G. Mellau[c]

[a] *Institute of Atmospheric Optics, Russian Academy of Sciences, 1, av. Akademicheskii, 634055, Tomsk, Russia*
[b] *Groupe de Spectrométrie Moléculaire et Atmosphérique, UMR CNRS 6089, Université de Reims, Faculté des Sciences, Moulin de la Housse, BP 1039, F-51687 Reims Cedex 2, France*
[c] *Justus-Liebig-Universitaet Giessen, Heinrich-Buff-Ring 58, D-35392 Giessen, Germany*

Received 12 July 2002; in revised form 6 September 2002

Abstract

The far-infrared emission spectrum of water vapour have been recorded at temperature 1370 K in the range 400–850 cm^{-1} at resolutions (FWHM) 0.0055 cm^{-1}. The measurements have been done in a fused quartz cell with an effective length of hot gas of about 60 cm. Among about 200 lines assigned to the $H_2{}^{18}O$ isotopomer 106 lines have not been reported in previous studies. These newly measured lines correspond to higher values of rotational quantum numbers compared to previous determinations: $J_{max} = 18$ and $K_{a\,(max)} = 17$ for the $(0\,0\,0) \leftarrow (0\,0\,0)$ band and $J_{max} = 15$ and $K_{a\,(max)} = 11$ for the $(0\,1\,0) \leftarrow (0\,1\,0)$ band. Estimated accuracy of line position measurements is 0.0005 cm^{-1}. To our knowledge rotational transitions within an excited bending state have been measured for the first time for $H_2{}^{18}O$. An extended set of experimental rotational energy levels for (0 0 0) and (0 1 0) vibration states including all previously available data has been determined. A data reduction has been done using the generating function model. The root mean square (RMS) deviation between observed and calculated values is 0.0009 cm^{-1} for 305 rotational levels of the (0 0 0) state and 0.0007 cm^{-1} for 198 rotational levels of the (0 1 0) state. A comparison of the observed data with the best available predictions from the molecular electronic potential energy surface [J. Chem. Phys. 106 (1997) 4618] and isotopic effects for rotational levels of (0 0 0) and (0 1 0) states are discussed.

Keywords: Far-infrared spectroscopy; Hot water; $H_2{}^{18}O$; Emission spectra; Non-rigid molecules; Centrifugal distortion; Rotational levels; Isotopic effects

1. Introduction

A detailed knowledge of line positions and energy levels of the water molecule and of its isotopic species is known to be important for various atmospheric and astrophysical applications of the spectroscopy. On the other hand spectroscopy of the water molecule stimulate theoretical studies of non-rigid molecules with extremely strong centrifugal distortion. The calculation of water rotational energies, especially for high K_a quantum number, is commonly considered a touchstone for many theoretical models. The aim of this study was to extend experimental information on rotational energy levels of $H_2{}^{18}O$ from an analysis of emission spectra of heated water vapour in the 400–850 cm^{-1} region and to study isotopic effects in observed and calculated levels.

The $H_2{}^{18}O$ is the second most abundant isotopomer of water after $H_2{}^{16}O$ and has been a subject of rather intensive studies. Rotational energies of the ground and first excited vibrational states of $H_2{}^{18}O$ has been determined by Fraley et al. [1] and Williamson et al. [2] through the analysis of spectra in the range of fundamental bands occurring in the near infrared at 5–7.5 μm and at 2.5–3.0 μm region. Few transitions in the v_2 band have been measured by Johns and McKeller [3] using the technique of intracavity CO laser Stark spectroscopy. The v_2 fundamental band has been studied more extensively at high resolution by Guelachvili [4], Camy-Peyret et al. [5], and Toth [6]. Pure rotational transitions

* Corresponding author. Fax: +33-3-26-91-31-47.
E-mail address: vladimir.tyuterev@univ-reims.fr (V.G. Tyuterev).

0022-2852/03/$ - see front matter © 2003 Elsevier Science (USA). All rights reserved.
doi:10.1016/S0022-2852(02)00018-8

in microwave spectra recorded by Steenbeckeliers and Bellet [7] and De Lucia et al. [8] and in far-infrared spectra recorded by Johns [9] in the 60–280 cm^{-1} region and by Kauppinen and Kyro [10] in the 67–695 cm^{-1} region have contributed to an accurate determination of rotational energy levels of $H_2{}^{18}O$ with relatively low-rotational J, K_a quantum numbers. New measurements of $(000) \leftarrow (000)$ rotational transitions have been recently reported by Toth [11] in 595–943 cm^{-1} region and by Matsushima et al. [12] in 18–172 cm^{-1} region. Spectra of $H_2{}^{18}O$ have been studied further in the region of the 1st triad [13–16] and the 2nd triad [17,18] and also in a higher wavenumber range [19–20].

Note that all experimentally available rotational levels [11] and almost all rovibrational levels of $H_2{}^{18}O$ were determined from analysis of room-temperature spectra and thus correspond to relatively moderate values of rotational quantum numbers J, K_a. The only hot $H_2{}^{18}O$ band analysed so far is the $(021) \leftarrow (010)$ band reported by Chevillard et al. [21]. Also some $H_2{}^{18}O$ v_3 line positions at 1200 K with natural isotopic abundance have been measured by Pine et al. [22]. The situation is quite different from that of the major isotopomer $H_2{}^{16}O$ for which a lot of information on high J, K_a energy levels has been deduced from hot water spectra (sf. for example [22–28] and references therein).

In this paper we report a first observation of rotational transitions $(010) \leftarrow (010)$ in the excited bending vibration state of $H_2{}^{18}O$ in water emission spectra recorded at 1370 K. Also new rotational transitions in the ground vibration state (000) have been assigned that allows to improve an accuracy of the determination of highly excited rotational levels and to extend considerably the range of experimentally accessible rotational quantum numbers for $H_2{}^{18}O$.

The data reduction has been done using the generating-function model [29–31] of the effective rotational Hamiltonian because the usual polynomial model for centrifugal distortion terms [32] employed in all previous analysis of $H_2{}^{18}O$ spectra [1–20] does not provide a satisfactory accuracy for our data. Comparisons of our experimental data and calculations with global predictions for (000) and (010) levels performed by Partridge and Schwenke [33] from an electronic potential energy surface, as well as isotopic shift variation versus J and K_a are discussed.

2. Experimental spectra analysis

The far-infrared emission spectrum of heated water vapour (with natural isotopic abundance) has been recorded at resolution 0.0055 cm^{-1} at Giessen on the Brucker IFS 120 HR Fourier transform spectrometer [34] which had been previously used to record room-temperature spectra of $D_2{}^{16}O$ [35] and $H_2{}^{16}O$ [28,36]. The measurements for the present work were done in a fused quartz cell with an effective length of hot gas of about 60 cm. The gas was at temperature of 1370 K although a small segment near the windows was at much lower temperature. A description of the cell and other experimental details have been given in papers on HCN emission spectra experiments [37,38] in similar experimental conditions. Table 1 lists the conditions used in the recording of the emission spectrum.

Because the water sample had a natural isotopic abundance, most of ~13 000 emission water lines recorded in the 400–850 cm^{-1} region in the present study belong to the $H_2{}^{16}O$ isotopomer. These lines together with previously available data had been used in [28] to improve an accuracy of a determination of some $H_2{}^{16}O$ rovibrational states. About 200 lines have been assigned to $(000) \leftarrow (000)$ and $(010) \leftarrow (010)$ bands of the $H_2{}^{18}O$ isotopomer.

Low-J, K_a transitions could be readily assigned using available database compilations [39], and associated line positions are in a good agreement with room-temperature measurements [10,11]. An assignment of higher J, K_a transitions corresponding to weak observed lines requires extrapolations based on theoretical calculations. Because the standard polynomial model of the effective Hamiltonian in the case of water-type non-rigid molecules has poor convergence and extrapolation properties, we have used the generating function model [29–31] outlined in the following section, in a similar way as in our previous work on $H_2{}^{16}O$ spectra [28,36]. The assignment of transitions has been done using step-by-step iterative extrapolations with increasing J and K_a quantum numbers. The calibration of line positions has been achieved using available literature data [10,11] as well as our previous measurements of $H_2{}^{16}O$ lines [28].

In Table 2 we give new line positions of $H_2{}^{18}O$ (for transitions which had not been observed in previously reported room-temperature spectra) together with their rotational assignments. The second column gives estimations (in 10^{-4} cm^{-1}) of absolute uncertainties in experimental line positions.

Table 1
Laboratory measurement conditions for emission FTIR spectra of water vapour

Spectrometer	Bruker IFS 120 HR
Gas temperature	1370 K
Total water pressure	1.6×10^3 Pa
Length of the cell	1 m
Diameter of the cell	6 cm
Length of hot zone	60 cm
Detector	Ge:Cu at 4 K
Filter	400–900 cm^{-1} at 4 K
Window	KBr
Resolution	0.0055 cm^{-1}

Table 2
New $H_2{}^{18}O$ lines observed in emission spectrum

Observed position	σ	Observed emittance	$O-C$	Upper state				Lower state			
				$v_1\,v_2\,v_3$	J	K_a	K_c	$v_1\,v_2\,v_3$	J	K_a	K_c
(a) (0 0 0) ← (0 0 0) *transitions*											
414.6743	5	0.043	−3	0 0 0	9	8	1	0 0 0	8	7	2
419.0664	5	0.020	10	0 0 0	10	7	3	0 0 0	9	6	4
418.8777	5	0.026	−2	0 0 0	10	7	4	0 0 0	9	6	3
439.2281	5	0.032	−5	0 0 0	10	8	2	0 0 0	9	7	3
439.2219	5	0.060	−3	0 0 0	10	8	3	0 0 0	9	7	2
456.6028	5	0.119	−7	0 0 0	10	9	2	0 0 0	9	8	1
471.2257	5	0.146	−8	0 0 0	10	10	1	0 0 0	9	9	0
547.7524	5	0.023	−3	0 0 0	11	4	8	0 0 0	10	1	9
416.4078	5	0.032	12	0 0 0	11	5	6	0 0 0	10	4	7
543.2684	5	0.021	4	0 0 0	11	5	7	0 0 0	10	2	8
442.8515	5	0.070	0	0 0 0	11	7	4	0 0 0	10	6	5
463.4088	5	0.051	−4	0 0 0	11	8	3	0 0 0	10	7	4
457.5228	5	0.032	−4	0 0 0	12	5	7	0 0 0	11	4	8
466.4398	5	0.025	0	0 0 0	12	7	5	0 0 0	11	6	6
505.5149	20	0.042	4	0 0 0	12	9	3	0 0 0	11	8	4
505.5092	5	0.120	2	0 0 0	12	9	4	0 0 0	11	8	3
534.0296	5	0.153	11	0 0 0	12	11	2	0 0 0	11	10	1
544.3549	5	0.169	−5	0 0 0	12	12	1	0 0 0	11	11	0
623.2937	5	0.021	5	0 0 0	13	5	9	0 0 0	12	2	10
441.8879	20	0.032	−4	0 0 0	13	6	8	0 0 0	12	5	7
490.1788	5	0.128	−2	0 0 0	13	7	6	0 0 0	12	6	7
484.9149	5	0.032	−1	0 0 0	13	7	7	0 0 0	12	6	6
510.0354	5	0.035	0	0 0 0	13	8	6	0 0 0	12	7	5
529.3096	5	0.035	−23	0 0 0	13	9	4	0 0 0	12	8	5
529.2881	5	0.021	0	0 0 0	13	9	5	0 0 0	12	8	4
545.4061	5	0.141	0	0 0 0	13	10	3	0 0 0	12	9	4
558.8406	5	0.122	5	0 0 0	13	11	2	0 0 0	12	10	3
569.7219	20	0.298	−8	0 0 0	13	12	1	0 0 0	12	11	2
578.0844	5	0.108	2	0 0 0	13	13	0	0 0 0	12	12	1
559.3041	10	0.022	14	0 0 0	14	5	9	0 0 0	13	4	10
668.8314	5	0.021	14	0 0 0	14	5	10	0 0 0	13	2	11
513.9257	5	0.025	−15	0 0 0	14	6	8	0 0 0	13	5	9
664.4677	5	0.021	17	0 0 0	14	6	9	0 0 0	13	3	10
514.7348	5	0.025	−4	0 0 0	14	7	7	0 0 0	13	6	8
719.3791	10	0.021	12	0 0 0	14	7	8	0 0 0	13	4	9
502.7224	5	0.032	2	0 0 0	14	7	8	0 0 0	13	6	7
533.3844	5	0.027	−7	0 0 0	14	8	6	0 0 0	13	7	7
532.1362	5	0.057	0	0 0 0	14	8	7	0 0 0	13	7	6
552.6054	5	0.023	−14	0 0 0	14	9	5	0 0 0	13	8	6
552.5208	5	0.075	2	0 0 0	14	9	6	0 0 0	13	8	5
569.2275	5	0.088	23	0 0 0	14	10	5	0 0 0	13	9	4
583.1719	5	0.108	6	0 0 0	14	11	4	0 0 0	13	10	3
594.5862	5	0.097	6	0 0 0	14	12	3	0 0 0	13	11	2
603.5554	5	0.095	14	0 0 0	14	13	2	0 0 0	13	12	1
610.0751	5	0.092	3	0 0 0	14	14	1	0 0 0	13	13	0
694.0695	5	0.021	−23	0 0 0	15	4	11	0 0 0	14	3	12
617.3893	15	0.021	0	0 0 0	15	5	10	0 0 0	14	4	11
555.1027	5	0.029	1	0 0 0	15	6	9	0 0 0	14	5	10
699.2696	20	0.030	20	0 0 0	15	6	10	0 0 0	14	3	11
452.9466	5	0.032	−9	0 0 0	15	6	10	0 0 0	14	5	9
541.1532	5	0.043	−19	0 0 0	15	7	8	0 0 0	14	6	9
516.7371	5	0.032	18	0 0 0	15	7	9	0 0 0	14	6	8
556.0914	5	0.052	−5	0 0 0	15	8	7	0 0 0	14	7	8
552.9179	5	0.023	8	0 0 0	15	8	8	0 0 0	14	7	7
575.3734	5	0.063	3	0 0 0	15	9	6	0 0 0	14	8	7
575.1055	5	0.021	14	0 0 0	15	9	7	0 0 0	14	8	6
592.5294	5	0.068	7	0 0 0	15	10	5	0 0 0	14	9	6
592.5136	5	0.024	13	0 0 0	15	10	6	0 0 0	14	9	5
606.9880	5	0.105	4	0 0 0	15	11	4	0 0 0	14	10	5
618.9167	5	0.097	−3	0 0 0	15	12	3	0 0 0	14	11	4

Table 2 (*continued*)

Observed position	σ	Observed emittance	$O-C$	Upper state				Lower state			
				$v_1\,v_2\,v_3$	J	K_a	K_c	$v_1\,v_2\,v_3$	J	K_a	K_c
628.4488	5	0.076	0	0 0 0	15	13	2	0 0 0	14	12	3
635.6308	30	0.050	−31	0 0 0	15	14	1	0 0 0	14	13	2
640.4363	5	0.070	−12	0 0 0	15	15	0	0 0 0	14	14	1
765.2243	15	0.021	−44	0 0 0	16	5	12	0 0 0	15	2	13
738.5161	20	0.021	−46	0 0 0	16	6	11	0 0 0	15	3	12
454.5252	5	0.032	−32	0 0 0	16	6	11	0 0 0	15	5	10
570.8129	5	0.021	−32	0 0 0	16	7	9	0 0 0	15	6	10
526.2036	5	0.032	−6	0 0 0	16	7	10	0 0 0	15	6	9
571.7254	5	0.052	2	0 0 0	16	8	9	0 0 0	15	7	8
597.6253	5	0.021	−3	0 0 0	16	9	7	0 0 0	15	8	8
596.8841	10	0.060	6	0 0 0	16	9	8	0 0 0	15	8	7
615.2653	5	0.026	−24	0 0 0	16	10	6	0 0 0	15	9	7
615.2147	30	0.143	16	0 0 0	16	10	7	0 0 0	15	9	6
630.2567	15	0.044	3	0 0 0	16	11	5	0 0 0	15	10	6
630.2536	5	0.152	3	0 0 0	16	11	6	0 0 0	15	10	5
642.6899	5	0.141	−25	0 0 0	16	12	5	0 0 0	15	11	4
652.7515	5	0.100	−19	0 0 0	16	13	4	0 0 0	15	12	3
660.5391	5	0.075	12	0 0 0	16	14	3	0 0 0	15	13	2
666.0742	5	0.048	73	0 0 0	16	15	2	0 0 0	15	14	1
669.2753	5	0.033	17	0 0 0	16	16	1	0 0 0	15	15	0
806.2560	5	0.021	269	0 0 0	17	4	13	0 0 0	16	3	14
737.8213	5	0.034	−9	0 0 0	17	5	12	0 0 0	16	4	13
655.6881	15	0.021	19	0 0 0	17	6	11	0 0 0	16	5	12
605.1724	5	0.021	11	0 0 0	17	7	10	0 0 0	16	6	11
602.7011	5	0.034	40	0 0 0	17	8	9	0 0 0	16	7	10
587.6652	5	0.020	−50	0 0 0	17	8	10	0 0 0	16	7	9
619.4510	5	0.021	−34	0 0 0	17	9	8	0 0 0	16	8	9
637.4225	5	0.028	−2	0 0 0	17	10	7	0 0 0	16	9	8
637.2627	5	0.021	12	0 0 0	17	10	8	0 0 0	16	9	7
652.9476	5	0.032	−4	0 0 0	17	11	6	0 0 0	16	10	7
652.9369	5	0.021	−3	0 0 0	17	11	7	0 0 0	16	10	6
665.8872	5	0.063	−22	0 0 0	17	12	5	0 0 0	16	11	6
676.4552	30	0.080	12	0 0 0	17	13	4	0 0 0	16	12	5
684.7872	5	0.093	25	0 0 0	17	14	3	0 0 0	16	13	4
690.9328	5	0.035	−162	0 0 0	17	15	2	0 0 0	16	14	3
694.9360	5	0.041	−56	0 0 0	17	16	1	0 0 0	16	15	2
696.6691	5	0.038	−10	0 0 0	17	17	0	0 0 0	16	16	1
532.6323	20	0.021	14	0 0 0	18	7	12	0 0 0	17	6	11
599.7988	5	0.021	−1	0 0 0	18	8	11	0 0 0	17	7	10
636.8756	5	0.039	−60	0 0 0	18	9	10	0 0 0	17	8	9
675.0376	5	0.026	−3	0 0 0	18	11	7	0 0 0	17	10	8
675.0044	5	0.038	0	0 0 0	18	11	8	0 0 0	17	10	7
688.4847	5	0.071	−3	0 0 0	18	12	7	0 0 0	17	11	6
699.5360	20	0.023	−5	0 0 0	18	13	6	0 0 0	17	12	5
708.3811	15	0.021	98	0 0 0	18	14	5	0 0 0	17	13	4
715.0971	15	0.021	−13	0 0 0	18	15	4	0 0 0	17	14	3
(b) (0 1 0) ← (0 1 0) *transitions*											
416.4196	5	0.032	−2	0 1 0	8	8	1	0 1 0	7	7	0
441.4611	5	0.021	−6	0 1 0	9	8	1	0 1 0	8	7	2
458.3014	5	0.032	3	0 1 0	9	9	0	0 1 0	8	8	1
445.4744	5	0.032	3	0 1 0	10	7	3	0 1 0	9	6	4
445.3629	5	0.032	1	0 1 0	10	7	4	0 1 0	9	6	3
466.1826	5	0.023	−4	0 1 0	10	8	3	0 1 0	9	7	2
483.4931	5	0.061	4	0 1 0	10	9	2	0 1 0	9	8	1
497.5954	5	0.074	1	0 1 0	10	10	1	0 1 0	9	9	0
446.1404	15	0.032	−18	0 1 0	11	6	5	0 1 0	10	5	6
469.3371	5	0.032	4	0 1 0	11	7	4	0 1 0	10	6	5
490.5236	5	0.027	2	0 1 0	11	8	3	0 1 0	10	7	4
490.5053	5	0.032	−1	0 1 0	11	8	4	0 1 0	10	7	3
508.3240	5	0.026	3	0 1 0	11	9	2	0 1 0	10	8	3
522.9247	5	0.035	2	0 1 0	11	10	1	0 1 0	10	9	2

Table 2 (*continued*)

Observed position	σ	Observed emittance	$O-C$	Upper state				Lower state			
				$v_1\,v_2\,v_3$	J	K_a	K_c	$v_1\,v_2\,v_3$	J	K_a	K_c
534.5378	10	0.032	2	0 1 0	11	11	0	0 1 0	10	10	1
399.3049	5	0.020	−32	0 1 0	12	5	8	0 1 0	11	4	7
458.6207	5	0.076	41	0 1 0	12	6	7	0 1 0	11	5	6
492.8576	20	0.026	6	0 1 0	12	7	5	0 1 0	11	6	6
491.6386	20	0.032	17	0 1 0	12	7	6	0 1 0	11	6	5
514.4060	20	0.020	−41	0 1 0	12	8	4	0 1 0	11	7	5
514.3407	20	0.020	20	0 1 0	12	8	5	0 1 0	11	7	4
532.7321	5	0.029	5	0 1 0	12	9	4	0 1 0	11	8	3
547.8407	5	0.025	1	0 1 0	12	10	3	0 1 0	11	9	2
559.9877	5	0.023	1	0 1 0	12	11	2	0 1 0	11	10	1
499.1862	5	0.032	24	0 1 0	13	6	7	0 1 0	12	5	8
516.2172	20	0.021	−45	0 1 0	13	7	6	0 1 0	12	6	7
556.6711	5	0.032	−15	0 1 0	13	9	4	0 1 0	12	8	5
572.3075	5	0.021	73	0 1 0	13	10	3	0 1 0	12	9	4
584.9628	5	0.021	1	0 1 0	13	11	2	0 1 0	12	10	3
532.3723	5	0.032	3	0 1 0	14	7	8	0 1 0	13	6	7
560.0346	5	0.023	7	0 1 0	14	8	7	0 1 0	13	7	6
580.0362	5	0.021	−138	0 1 0	14	9	6	0 1 0	13	8	5
596.2389	5	0.021	−218	0 1 0	14	10	5	0 1 0	13	9	4
609.4180	5	0.023	−70	0 1 0	14	11	4	0 1 0	13	10	3
583.2269	5	0.022	0	0 1 0	15	8	7	0 1 0	14	7	8
602.9489	5	0.021	2	0 1 0	15	9	6	0 1 0	14	8	7

Note. Observed line positions are given in cm^{-1}. σ, the error estimation of the line experimental line position, in units $10^{-4}\,cm^{-1}$. Observed emittance is in arbitrary units. $O-C$, deviation between the observed line position and our calculated line position using parameters of Table 4, in units $10^{-4}\,cm^{-1}$.

3. Data reduction: energy levels and hamiltonian parameters for (0 0 0) and (0 1 0) states

To assure a consistency with calibrations of previous works on water spectra [1–21], and a self-consistency of energy level determinations from various sources of experimental line positions, we have applied the RITZ code written by Tashkun et al. [40] in a similar way as in our recent study on $H_2{}^{16}O$ spectra [28]. This used the RITZ combination principle to recover all possible energy levels by simultaneous processing of line positions in various records over an interval which extended beyond that which is the focus of this work. This procedure accounts for our own measured line positions together with complementary literature data to generate a set of energy levels which provide transition wavenumbers in agreement with observations according to a least squares procedure. In cases where a level is involved in many observed transitions the program provides for averaging, which eliminates to a certain extent contributions of line shifts and gives more reliable experimental estimates than a classical combination difference approach. A detailed description of this technique applied to various molecules will be discussed elsewhere [40].

A total of 3937 observed transitions including those of [6,8–12,15,16,19,21] were simultaneously used to obtain a new set of rotational energies for (0 0 0) and (0 1 0) vibration states of $H_2{}^{18}O$. The results of energy level determinations achieved with this procedure are presented in Table 3 in comparison with the most complete previous set of [11]. The column headed "N_t" indicates number of observed transitions involved in the determination of each level. A statistical analysis of the obtained data set, performed with the RITZ-program [40], indicates that information from microwave transitions [8] and particularly from very accurate recent measurements of Matsushima et al. [12] in 1–5 THz region contributes significantly to precise determination of low-J levels, whereas complementary information from our high-temperature spectra allow to determine higher rotational energies.

It is well known that an accurate calculation of excited rotational states of the water molecule and of related analysis of high-resolution spectra is complicated by an extremely strong centrifugal distortion resulting from the bending-rotational coupling. Because of this coupling the standard power series expansion of the effective rotational Hamiltonian H_{rot} used in previous papers pertaining to the assignment of the $H_2{}^{18}O$ spectra has a limited domain of validity. According to estimations [29] of the convergence radius of this expansion, the domain of its applicability is limited by a maximal value $K_{a\,max}$ which depends on v_2. For (0 0 0) and (0 1 0) states of the water molecule the convergence radii of the power series expansion of H_{rot} correspond to $K_{a\,max} = 11$ and $K_{a\,max} = 9$, but we have observed transitions with higher values of K_a: up to 17 in the case

Table 3
Experimentally determined rotation energies of (0 0 0) and (0 1 0) vibration states of $H_2{}^{18}O$

J	K_a	K_c	(0 0 0) State					(0 1 0) State				
			E_{obs}/hc	δ_{obs}	N_t	Obs − Cal	Obs − [11]	E_{obs}/hc	δ_{obs}	N_t	Obs − Cal	Obs − [11]
1			2	3	4	5	6	2	3	4	5	6
0	0	0	0					1588.27563	.16	2	.00	−.04
1	0	1	23.75490	.02	21	.03	.00	1612.04599	.13	4	.03	−.02
1	1	1	36.74859	.03	22	−.18	−.06	1628.06007	.11	6	.11	.01
1	1	0	42.02341	.02	20	−.07	−.02	1633.63470	.15	3	.10	−.01
2	0	2	69.92736	.03	26	−.01	−.08	1658.33384	.08	7	−.06	−.06
2	1	2	78.98863	.02	35	−.13	−.02	1670.03713	.11	7	.08	.02
2	1	1	94.78855	.03	25	−.04	−.10	1686.73330	.08	6	.08	−.07
2	2	1	133.47580	.02	30	−.10	.00	1734.21855	.09	8	.13	.03
2	2	0	134.78304	.03	29	−.17	−.08	1735.43765	.09	6	−.04	−.09
3	0	3	136.33667	.02	42	.07	.00	1725.01686	.07	8	−.05	−.03
3	1	3	141.56799	.03	36	−.16	−.07	1732.26271	.07	8	.00	−.06
3	1	2	172.88291	.02	39	.14	.00	1765.39797	.08	8	.09	−.04
3	2	2	204.75584	.03	34	−.11	−.07	1805.57662	.06	8	−.02	−.09
3	2	1	210.79925	.02	45	−.02	−.03	1811.29059	.08	8	.00	−.03
3	3	1	282.09453	.03	28	.05	−.05	1897.45280	.05	9	−.25	−.02
3	3	0	282.30712	.02	31	.12	.03	1897.62728	.07	8	−.17	.04
4	0	4	221.23389	.02	36	−.09	−.12	1810.18727	.09	8	−.10	−.05
4	1	4	223.82851	.02	41	−.09	−.05	1814.08713	.05	8	.04	−.03
4	1	3	274.80317	.02	33	.19	−.04	1868.25382	.03	9	.08	−.03
4	2	3	298.62016	.02	46	.02	−.02	1899.60893	.04	11	.05	−.01
4	2	2	314.45937	.02	42	−.03	−.09	1914.88087	.06	8	−.11	−.04
4	3	2	379.29164	.02	46	.07	.02	1994.70331	.06	11	−.18	.00
4	3	1	380.70248	.03	31	.02	−.04	1995.87007	.03	7	−.31	−.06
4	4	1	482.64365	.05	24	.18	.08	2117.00851	.06	9	.03	.02
4	4	0	482.67261	.03	28	.07	−.01	2117.02965	.09	6	−.04	−.06
5	0	5	324.04672	.02	39	−.04	−.03	1913.02263	.04	9	−.01	−.01
5	1	5	325.21569	.02	34	−.10	−.05	1914.93344	.05	9	.01	−.08
5	1	4	398.36049	.02	44	.21	−.03	1993.27685	.08	10	.02	−.04
5	2	4	414.16813	.02	38	.02	−.06	2015.45390	.07	9	.05	−.06
5	2	3	445.15853	.02	47	.05	−.05	2045.92261	.08	10	−.20	−.06
5	3	3	500.59625	.02	36	.04	−.02	2116.13852	.07	10	−.25	−.06
5	3	2	505.72883	.02	48	.04	−.01	2120.45465	.08	10	−.24	.00
5	4	2	604.54420	.02	35	.01	−.02	2238.97487	.05	9	.09	−.08
5	4	1	604.79296	.02	37	.08	.02	2239.15709	.05	10	.19	.04
5	5	1	733.67938	.03	12	−.17	−.01	2390.35364	.03	4	.36	.06
5	5	0	733.68318	.02	21	−.07	.08	2390.35607	.06	5	.37	−.01
6	0	6	444.84621	.02	28	−.02	−.02	2033.48861	.06	8	−.06	−.09
6	1	6	445.34619	.02	39	−.07	−.04	2034.37686	.05	10	.02	−.05
6	1	5	541.18006	.02	31	.12	−.11	2138.08857	.05	8	.04	−.02
6	2	5	550.45078	.02	38	.06	−.07	2152.18203	.06	11	.10	−.09
6	2	4	601.23775	.02	36	.02	−.11	2202.99269	.03	8	−.22	−.06
6	3	4	645.38254	.02	42	.00	−.09	2261.21754	.06	11	−.11	.01
6	3	3	658.61006	.02	39	−.04	−.04	2272.64610	.09	8	−.29	−.04
6	4	3	751.03306	.02	46	.11	.05	2385.51357	.06	11	.17	.00
6	4	2	752.18744	.03	36	−.01	−.08	2386.36584	.06	9	.08	−.03
6	5	2	880.07644	.02	27	−.08	.08	2536.90968	.05	7	.81	.01
6	5	1	880.11451	.03	30	−.30	−.12	2536.93482	.03	7	.78	−.07
6	6	1	1033.19417	.03	15	−.20	.03	2714.44446	.09	5	.11	.10
6	6	0	1033.19450	.03	6	−.33	−.06	2714.44446	.04	2	−.17	.00
7	0	7	583.77783	.02	34	−.04	.03	2171.74067	.07	8	.05	−.07
7	1	7	583.98642	.02	26	−.08	−.11	2172.14323	.07	7	.12	−.01
7	1	6	701.69426	.02	39	.13	−.07	2300.77431	.05	10	.00	.04
7	2	6	706.59781	.02	37	.16	−.02	2308.90599	.08	7	.15	−.07
7	2	5	780.45278	.02	41	−.06	−.08	2384.04190	.04	9	−.23	−.09
7	3	5	812.76174	.03	33	.15	−.02	2429.13499	.03	8	.00	−.05
7	3	4	839.54949	.02	40	−.05	−.05	2453.05766	.05	9	−.07	.03
7	4	4	921.89593	.03	30	.11	.03	2556.46209	.03	8	.06	−.08
7	4	3	925.69992	.02	36	.22	.09	2559.31394	.04	8	.07	−.05
7	5	3	1050.99035	.03	28	−.03	.05	2707.92161	.03	6	.52	−.12

Table 3 (*continued*)

J	K_a	K_c	(0 0 0) State					(0 1 0) State				
			E_{obs}/hc	δ_{obs}	N_t	Obs – Cal	Obs – [11]	E_{obs}/hc	δ_{obs}	N_t	Obs – Cal	Obs – [11]
1			2	3	4	5	6	2	3	4	5	6
7	5	2	1051.20319	.06	33	−.04	−.07	2708.06223	.02	8	.67	.00
7	6	2	1204.16934	.03	14	−.52	−.17	2885.71706	.07	3	.30	−.15
7	6	1	1204.17485	.06	23	−.52	−.11	2885.72059	.03	3	.53	−.04
7	7	1	1378.98670	.10	7	.53	.27	3086.18835	.16	2	−.95	.09
7	7	0	1378.98670	.08	13	.47	.27	3086.18835	.14	3	−.98	.09
8	0	8	740.91235	.03	25	.03	.00	2327.88503	.08	7	.08	−.05
8	1	8	740.99870	.02	27	.07	−.04	2328.06612	.08	8	.27	.10
8	1	7	879.49470	.03	31	−.06	−.17	2480.50567	.02	6	−.08	−.03
8	2	7	881.91426	.02	37	.31	.11	2484.87714	.04	8	.08	−.14
8	2	6	980.22231	.03	30	−.12	−.07	2586.63348	.03	6	−.14	−.11
8	3	6	1001.70572	.02	34	.10	−.14	2618.92131	.04	8	.25	−.03
8	3	5	1047.32855	.06	26	−.26	−.10	2661.00402	.02	7	.22	−.02
8	4	5	1116.63623	.02	36	.02	.00	2751.41840	.03	8	.14	−.14
8	4	4	1126.43911	.07	26	.12	−.05	2758.96007	.02	6	.13	−.09
8	5	4	1246.36855	.02	30	−.03	.00	2903.32970	.03	7	.29	.04
8	5	3	1247.20612	.07	22	.20	−.04	2903.88637	.04	6	.25	−.06
8	6	3	1399.42818	.05	25	.01	.12	3081.20090	.06	5	.02	−.11
8	6	2	1399.46303	.10	16	−.48	−.33	3081.22212	.07	5	.08	−.03
8	7	2	1574.67821	.08	13	.06	.21	3282.34232	.10	5	−.32	.36
8	7	1	1574.67851	.09	6	−.41	.06	3282.34237	.09	2	−.69	−.27
8	8	1	1768.80173	.11	7	.94	.25	3502.60798	.14	5	−.66	.17
8	8	0	1768.80173	.15	4	.94	.25	3502.60798	.28	*	−.66	.17
9	0	9	916.25780	.03	23	.11	.01	2501.95934	.07	6	.18	−.02
9	1	9	916.29353	.06	22	.06	−.07	2502.04076	.09	6	.04	−.07
9	1	8	1074.76294	.03	33	−.06	−.14	2677.28337	.07	8	−.16	−.04
9	2	8	1075.90944	.06	26	.07	−.08	2679.53346	.05	6	−.16	−.13
9	2	7	1198.19950	.03	31	−.30	−.16	2808.28013	.03	6	−.22	−.20
9	3	7	1211.18563	.06	22	.22	−.13	2829.56103	.04	6	.45	−.05
9	3	6	1279.79751	.03	21	−.49	−.16	2894.70558	.02	6	.41	−.08
9	4	6	1334.47936	.06	20	−.02	.01	2969.72197	.05	7	.29	−.08
9	4	5	1355.19908	.05	23	.05	−.08	2986.25894	.03	7	.25	−.19
9	5	5	1466.01848	.08	13	.17	.11	3122.96940	.07	5	−.33	−.12
9	5	4	1468.61209	.05	25	.41	−.12	3124.71634	.05	6	.05	−.15
9	6	4	1618.89618	.08	14	.02	−.16	3300.78714	.09	5	−.47	−.01
9	6	3	1619.05608	.05	20	.56	.21	3300.88270	.09	7	−.62	−.34
9	7	3	1794.37509	.14	6	.15	.34	3502.42260	.12	2	−1.34	−.25
9	7	2	1794.38018	.07	10	−.31	−.27	3502.42622	.12	4	−.78	.21
9	8	2	1989.35209	1.00	1	−.68	.14	3723.80350	.30	*	−.24	−.54
9	8	1	1989.35209	.11	9	−.79	.14	3723.80350	.15	5	−.30	−.54
9	9	1	2200.40578	.30	*	.52	.43	3960.90911	.46	*	1.73	.11
9	9	0	2200.40578	.15	3	.52	.43	3960.90911	.23	4	1.73	.11
10	0	10	1109.78693	.08	14	.01	−.15	2693.95588	.09	3	−.21	−.29
10	1	10	1109.80210	.06	19	.21	−.01	2693.99334	.11	6	.03	−.04
10	1	9	1287.73457	.08	18	−.32	−.28	2891.35965	.09	4	−.37	−.12
10	2	9	1288.26732	.06	27	.14	−.03	2892.49206	.05	6	−.20	−.10
10	2	8	1433.02898	.11	13	−.06	−.01	3047.09222	.08	5	−.27	−.16
10	3	8	1440.28795	.06	24	.26	−.11	3060.10388	.05	7	.46	−.10
10	3	7	1534.36830	.10	10	−.70	−.07	3151.80967	.11	5	.56	−.06
10	4	7	1574.44940	.06	21	−.32	−.17	3210.49921	.05	7	.47	−.10
10	4	6	1611.65347	.11	12	−.07	−.10	3241.48621	.09	5	.52	−.02
10	5	6	1709.54016	.07	16	−.19	.40	3366.51770	.06	8	−.85	−.16
10	5	5	1716.19997	.10	10	.89	.45	3371.09888	.09	5	.12	−.10
10	6	5	1862.45478	.08	13	−.01	−.10	3544.33419	.12	6	−.66	−.28
10	6	4	1863.01995	.12	10	.38	.15	3544.67626	.14	3	.07	.06
10	7	4	2037.93390	.09	8	.35	−.05	3746.24525	.13	5	−.91	−.12
10	7	3	2037.96234	.15	8	.83	.34	3746.26090	.16	4	−.64	−.08
10	8	3	2233.60249	.13	6	.04	−.16	3968.60891	.22	3	−.27	−.54
10	8	2	2233.60330	.14	3	.00	.15	3968.61053	1.00	1	.91	.28
10	9	2	2445.95489	.14	4	−1.28	.39	4207.29643	.38	2	1.88	−1223.86
10	9	1	2445.95489	.28	*	−1.29	.39	4207.29643	.76	*	1.87	−1223.86

Table 3 (*continued*)

J	K_a	K_c	(0 0 0) State					(0 1 0) State				
			E_{obs}/hc	δ_{obs}	N_t	Obs − Cal	Obs − [11]	E_{obs}/hc	δ_{obs}	N_t	Obs − Cal	Obs − [11]
1			2	3	4	5	6	2	3	4	5	6
10	10	1	2671.63141	.32	3	−.93	1.56	4458.50430	.42	2	−1.36	−9321.65
10	10	0	2671.63141	.64	*	−.93	1.56	4458.50430	.82	*	−1.36	−9321.65
11	0	11	1321.45464	.10	14	.61	.30	2903.84381	.10	3	.24	.01
11	1	11	1321.45993	.13	9	−.45	−.59	2903.86072	.12	3	−.17	−.20
11	1	10	1518.54253	.09	16	−.07	−.05	3122.94152	.09	4	.06	.13
11	2	10	1518.78765	.13	10	−.33	−.34	3123.50588	.12	3	−.48	−.13
11	2	9	1684.43939	.09	14	.13	−.05	3302.22934	.09	5	−.09	−.08
11	3	9	1688.28634	.12	10	.42	−.10	3309.74530	.11	4	.54	−.05
11	3	8	1808.36231	.09	13	−.68	−.04	3429.72568	.08	5	.26	−.09
11	4	8	1835.48675	.14	14	−.31	−.05	3472.75127	.13	4	.14	−.20
11	4	7	1894.19573	.10	11	−.40	−.04	3523.74045	.08	4	−.37	−.05
11	5	7	1976.29750	.13	8	−.11	.27	3633.45135	.11	4	−2.19	−.20
11	5	6	1990.85695	.10	12	.95	.15	3643.79517	.14	6	.08	−.15
11	6	6	2129.89790	.11	8	−.60	.08	3811.64173	.17	3	−.04	.11
11	6	5	2131.56623	.11	8	.51	.03	3812.65798	.94	2	−1.74	−22.02
11	7	5	2305.19472	.13	4	−1.03	−1.28	4013.61029	.27	2	.73	−.32
11	7	4	2305.30620	.15	7	.17	.00	4013.67122	.22	3	.87	−.21
11	8	4	2501.3418 e	.24	2	4.27	−110.93	4236.76638	.22	2	.24	−.37
11	8	3	2501.34271	.35	2	.41	−114.61	4236.76869	.25	3	.17	−.26
11	9	3	2714.86265	.58	*	.94	−1.15	4476.93274	.86	*	1.01	−937.86
11	9	2	2714.86265	.29	2	.81	−2.23	4476.93274	.43	2	.95	−937.86
11	10	2	2942.31325	.62	*	−.35		4730.22092	1.10	*	−.94	
11	10	1	2942.31325	.31	2	−.35		4730.22092	.55	2	−.94	
11	11	1	3180.40686	.90	*	−.29		4993.04184	2.00	*	.43	
11	11	0	3180.40686	.45	2	−.29		4993.04184	1.00	1	.43	
12	0	12	1551.20192	.18	9	.16	−.20	3131.57453	.15	3	−.56	−.65
12	1	12	1551.20495	.14	12	.45	−.01	3131.58354	.12	3	.14	.15
12	1	11	1767.22493	.17	7	−.56	−.18	3372.13535	.14	3	.03	−.17
12	2	11	1767.33885	.13	11	.03	.20	3372.41748	.12	4	−.08	.07
12	2	10	1952.67784	.16	8	.12	−.31	3573.67535	.18	2	.02	−.09
12	3	10	1954.65355	.11	12	.46	−.01	3577.86092	.11	4	.18	.02
12	3	9	2099.56272	.24	6	−.42	.17	3725.96582	1.00	1	−.59	−.08
12	4	9	2116.56478	.13	10	−.21	−.08	3755.45791	.10	4	−.10	.01
12	4	8	2200.43789	.22	3	−.58	−.99					
12	5	8	2265.43902	.18	4	−.03	.65	3923.0464 e	.17	4	−4.91	.09
12	5	7	2293.00958	.24	3	.12	−.62	3943.49842	1.00	1	−1.04	−.08
12	6	7	2420.88534	.12	7	−.64	.14	4102.41570	.32	2	2.39	372.60
12	6	6	2425.12367	.16	4	.76	−.03					
12	7	6	2595.97487	.16	3	−1.05	−.32	4304.29645	1.55	1	−.47	643.85
12	7	5	2596.33807	.19	3	.25	−.23	4304.49920	2.00	1	1.93	632.98
12	8	5	2792.33816	.29	2	.34	−2.84	4528.01177	1.64	2	2.41	744.87
12	8	4	2792.35668	.20	3	−1.37	.45	4528.01615	2.00	1	−3.47	
12	9	4	3006.85190	.58	2	1.14	4.70	4769.50062	.49	2	.24	
12	9	3	3006.8568 e	1.00	1	5.23	8.76	4769.50062	.98	*	−.13	
12	10	3	3235.96129	.40	2	−.28		5024.77323	.61	2	−1.85	
12	10	2	3235.96129	.80	*	−.30		5024.77323	1.22	*	−1.86	
12	11	2	3476.34286	.45	2	1.09		5290.20846	.72	2	.14	
12	11	1	3476.34286	.90	*	1.09		5290.20846	1.44	*	.14	
12	12	1	3724.76172	.64	2	−.69						
12	12	0	3724.76172	.64	*	−.69						
13	0	13	1798.96531	.18	10	.30	−.18	3377.09600	.21	2	.87	.46
13	1	13	1798.96508	.23	6	−1.14	−1.29	3377.09917	.22	2	−.13	−.09
13	1	12	2033.76607	.22	8	.13	.37	3638.97564	.16	2	.80	−.13
13	2	12	2033.81693	.27	5	−1.83	−1.29	3639.11695	.20	3	−.24	−.15
13	2	11	2238.03206	.15	10	1.03	.06	3861.71649	.16	3	.84	.04
13	3	11	2239.02983	.23	5	.22	−.04	3863.99980	.19	2	−.81	−.55
13	3	10	2406.77011	.15	7	1.36	.22	4038.65464	.15	2	.14	−.12
13	4	10	2416.78334	.20	4	.00	.54	4057.66668	1.00	1	−.46	.13
13	4	9	2527.68873	.21	3	−.44	−.14					
13	5	9	2575.97153	.19	3	−1.08	−.22					
13	5	8	2622.00999	.16	2	.84	.72					

Table 3 (*continued*)

J	K_a	K_c	(0 0 0) State					(0 1 0) State				
			E_{obs}/hc	δ_{obs}	N_t	Obs – Cal	Obs – [11]	E_{obs}/hc	δ_{obs}	N_t	Obs – Cal	Obs – [11]
1			2	3	4	5	6	2	3	4	5	6
13	6	8	2734.89689	.30	3	−3.11	.92					
13	6	7	2744.34538	.19	3	.33	−.18	4422.23241	.38	2	1.17	529.21
13	7	7	2910.03916	.27	3	.32	−1.42					
13	7	6	2911.06386	.21	3	.03	.40	4618.63276	1.44	2	−.26	
13	8	6	3106.37348	.42	2	.16	−14.52					
13	8	5	3106.44666	.24	3	1.02	1.39					
13	9	5	3321.64477	1.00	1	−1.42						
13	9	4	3321.64760	.39	2	−2.17		5084.68270	1.73	2	1.07	
13	10	4	3552.25797	1.54	*	1.27		5341.8084 e	1.38	*	8.10	
13	10	3	3552.25797	.77	2	1.14		5341.8084 e	.69	2	8.04	
13	11	3	3794.80192	1.06	*	.24		5609.73587	2.00	*	.88	
13	11	2	3794.80192	.53	2	.24		5609.73587	1.00	1	.88	
13	12	2	4046.06474	3.16	*	.22						
13	12	1	4046.06474	1.58	2	.22						
13	13	1	4302.84613	1.64	*	.41						
13	13	0	4302.84613	.82	2	.41						
14	0	14	2064.67217	.26	6	−.07	−.08	3640.34209	1.00	1	.42	−.18
14	1	14	2064.67325	.23	8	.47	.34	3640.34329	.27	3	−.64	−.15
14	1	13	2318.11350	.31	5	−.60	−.17	3923.44772	.33	1	−.64	−1.30
14	2	13	2318.13791	.52	3	−1.24	−.74	3923.52235	1.00	1	.89	.40
14	2	12	2540.66999	1.00	1	−.41	−1.16					
14	3	12	2541.17273	.23	4	−.13	.08	4167.85024	1.00	1	−1.13	−.02
14	3	11	2729.76584	.31	2	−.15	−2.96					
14	4	11	2735.41974	.27	2	1.70	.53	4378.55945	1.00	1	1.27	.16
14	4	10	2873.32317	1.00	1	2.55	.10					
14	5	10	2906.86346	.37	2	1.23	14.46					
14	5	9	2976.08795	.59	2	1.60						
14	6	9	3071.23779	.41	2	.96	18.90					
14	6	8	3089.89726	.41	2	−.76						
14	7	8	3247.06781	.36	3	−.55	20.77	4954.60453	.56	2	−1.54	
14	7	7	3249.63173	.44	2	−1.52						
14	8	7	3443.20007	.47	2	−.14		5178.66720	1.53	2	−1.50	
14	8	6	3443.42357	.50	2	.34						
14	9	6	3658.96746	.46	2	.97						
14	9	5	3658.97888	.62	2	−1.39						
14	10	5	3890.87507	.53	2	−.43		5680.9221 e	1.79	1	−12.57	
14	10	4	3890.87507	1.06	*	−1.05		5680.9221 e	3.58	*	−12.84	
14	11	4	4135.42990	.94	2	1.15		5951.22574	1.00	1	−.17	
14	11	3	4135.42990	1.88	*	1.13		5951.22574	2.00	*	−.18	
14	12	3	4389.38810	.68	2	.06						
14	12	2	4389.38810	1.36	*	.06						
14	13	2	4649.62016	1.67	2	1.14						
14	13	1	4649.62016	3.34	*	1.14						
14	14	1	4912.92118	1.00	2	1.08						
14	14	0	4912.92118	2.00	*	1.08						
15	0	15	2348.24641	.27	7	.31	−.07	3921.24784	.28	2	.40	−.06
15	1	15	2348.2456 e	.33	5	−.81	−.95	3921.24784	.56	*	−.96	−.26
15	1	14	2620.20327	.49	2	1.98	30.27	4225.51938	1.00	1	.64	−.26
15	2	14	2620.21433	1.00	1	.79	26.33	4225.55689	1.00	1	−.51	−.18
15	2	13	2860.65722	.27	2	.67	.51	4488.52335	1.00	1	−.15	.03
15	3	13	2860.90859	1.00	1	−1.93	.09					
15	3	12	3068.81808	1.45	1	2.56	−4.10					
15	4	12	3071.92687	1.00	1	.96	.00					
15	4	11	3235.24224	1.00	1	−3.83	−1.42					
15	5	10	3352.80902	1.32	2	−1.17	−20.19					
15	6	10	3429.03500	.68	3	−.09	35.20					
15	6	9	3461.96617	.57	2	1.49						
15	7	9	3606.63440	1.00	1	.34						
15	7	8	3612.39094	.62	2	1.32						
15	8	8	3802.54963	.60	2	−.74						
15	8	7	3803.15922	.53	2	.51		5537.83127	1.00	1	.85	

Table 3 (*continued*)

J	K_a	K_c	(0 0 0) State					(0 1 0) State				
			E_{obs}/hc	δ_{obs}	N_t	Obs – Cal	Obs – [11]	E_{obs}/hc	δ_{obs}	N_t	Obs – Cal	Obs – [11]
1			2	3	4	5	6	2	3	4	5	6
15	9	7	4018.52907	.71	2	1.65						
15	9	6	4018.57347	.63	2	.48		5781.61591	1.60	1	.30	
15	10	6	4251.49245	.77	2	−.54						
15	10	5	4251.49683	.68	2	1.28						
15	11	5	4497.86311	1.38	*	−.56						
15	11	4	4497.86311	.69	2	−.67						
15	12	4	4754.34659	2.24	*	−.03						
15	12	3	4754.34659	1.12	2	−.04						
15	13	3	5017.83693	1.66	*	−.73						
15	13	2	5017.83693	.83	2	−.73						
15	14	2	5285.25091	6.54	*	−2.81						
15	14	1	5285.25091	3.27	2	−2.81						
15	15	1	5553.35746	2.34	*	−.88						
15	15	0	5553.35746	1.17	2	−.88						
16	0	16	2649.60314	.41	2	−.69	−1.67	4219.74127	2.00	*	.70	−.04
16	1	16	2649.60430	.30	4	.30	−.51	4219.74127	1.00	1	−.27	−.04
16	2	14	3197.97471	1.00	1	−1.72	−1.29					
16	3	14	3198.0793 e	.33	2	−27.33	−.47					
16	4	13	3425.91891	.53	2	2.32	30.45					
16	5	12	3625.88154	1.06	2	−2.96	84.83					
16	6	11	3807.33419	1.44	3	−3.09						
16	7	10	3988.16976	.72	2	1.70						
16	7	9	3999.84787	.81	2	−2.06						
16	8	9	4184.11632	.80	2	1.78						
16	9	8	4400.04331	.90	2	1.14						
16	9	7	4400.17492	.76	2	−.50						
16	10	7	4633.78814	2.72	2	1.88						
16	10	6	4633.79434	.90	2	−.90						
16	11	6	4881.75047	.87	2	1.54						
16	11	5	4881.74919	1.50	1	−.21						
16	12	5	5140.55300	.81	2	−3.09						
16	12	4	5140.55300	1.62	*	−3.11						
16	13	4	5407.09812	1.29	2	−1.52						
16	13	3	5407.09812	2.58	*	−1.52						
16	14	3	5678.37599	1.00	2	1.38						
16	14	2	5678.37599	2.00	*	1.38						
16	15	2	5951.3247 e	3.35	2	4.84						
16	15	1	5951.3247 e	6.70	*	4.84						
16	16	1	6222.63276	1.35	2	.34						
16	16	0	6222.63276	2.70	*	.34						
17	0	17						4535.74522	1.00	1	.36	−.49
17	1	17						4535.74522	2.00	*	−.45	−.49
17	4	13	4004.33559	1.00	1	−.54						
17	5	12	4163.74021	1.00	1	1.05						
17	6	11	4281.56959	1.66	2	−.41						
17	7	10	4412.50661	1.54	2	.10						
17	8	10	4587.5123 e	1.00	1	−7.44						
17	8	9	4590.8707 e	.89	2	7.02						
17	9	8	4803.56731	1.00	1	−1.65						
17	10	8	5037.43758	.94	2	−.05						
17	10	7	5037.46578	1.05	2	.31						
17	11	7	5286.73127	1.05	1	−1.28						
17	11	6	5286.73577	2.81	2	1.48						
17	12	6	5547.63766	2.06	*	.24						
17	12	5	5547.63766	1.03	2	.15						
17	13	5	5817.00823	5.08	*	.02						
17	13	4	5817.00823	2.54	2	.02						
17	14	4	6091.88529	2.92	*	3.53						
17	14	3	6091.88529	1.46	2	3.53						
17	15	3	6369.3087 e	2.32	*	−12.49						
17	15	2	6369.3087 e	1.16	1	−12.49						

Table 3 (*continued*)

J	K_a	K_c	(0 0 0) State					(0 1 0) State				
			E_{obs}/hc	δ_{obs}	N_t	Obs – Cal	Obs – [11]	E_{obs}/hc	δ_{obs}	N_t	Obs – Cal	Obs – [11]
1			2	3	4	5	6	2	3	4	5	6
17	16	2	6646.26112	6.82	*	.28						
17	16	1	6646.26112	3.41	1	.28						
17	17	1	6919.30188	3.02	*	−.15						
17	17	0	6919.30188	1.51	1	−.15						
18	7	12	4814.20190	2.02	1	2.11						
18	8	11	5012.30542	1.62	1	−.47						
18	9	10	5227.74643	1.04	1	−.52						
18	11	8	5712.47021	1.19	1	−.55						
18	11	7	5712.47521	1.09	1	−1.21						
18	12	7	5975.22046	2.87	1	1.13						
18	12	6	5975.22046	5.74	*	.80						
18	13	6	6247.17369	2.00	1	−.07						
18	13	5	6247.17369	4.00	*	−.08						
18	14	5	6525.3893 e	2.85	1	9.25						
18	14	4	6525.3893 e	5.70	*	9.25						
18	15	4	6806.98239	1.73	1	−1.66						
18	15	3	6806.98239	3.46	*	−1.66						

Note. E_{obs}/hc, experimental term values in cm^{-1}; levels labeled with (e) in the next column are excluded from the fit (blended or very weak transitions: see the text). δ_{obs}, standard error of experimental value in $10^{-3}\,cm^{-1}$. N_t, number of observed transitions used to define the energy level. Transitions to those levels indicated by * in this column were not resolved. The energy for such levels were fixed to those of observed coincident partners. Obs – Calc, difference between observed and calculated term values, in $10^{-3}\,cm^{-1}$. Column 6: Obs – [11], difference between our observed term values and those of [11], in $10^{-3}\,cm^{-1}$.

of (0 0 0) and 11 in the case of (0 1 0). In order to account for the anomalous centrifugal distortion at high-rotational energies, we use in the present study the generating function model [29,30] which was shown to allow more accurate calculations [28,31,36].

The reduced effective rotational Hamiltonian for an isolated vibration state of an asymmetric top molecule is written in the form

$$H_{rot} = {}^{d}H_{rot} + {}^{nd}H_{rot}. \tag{1}$$

The diagonal ${}^{d}H_{rot}$ and the non-diagonal ${}^{nd}H_{rot}$ parts of the Hamiltonian relative to $|J,K\rangle$ wavefunctions are expanded in the generating function **G** following [30]:

$${}^{d}H_{v_1v_2v_3} = \sum_{nm} g_{nm}\mathbf{J}^{2n}\left\{\mathbf{G}(\alpha^{(J)})\right\}^{m}, \tag{2}$$

$${}^{nd}H_{v_1v_2v_3} = \sum_{nm} u_{nm}\mathbf{J}^{2n}\left[\left(J_+^2 + J_-^2\right), \left\{\mathbf{G}(\beta^{(J)})\right\}^{m}\right]_+, \tag{3}$$

where the generating function is defined according to [29]

$$\mathbf{G} \equiv \mathbf{G}(\alpha^{(J)}) = (2/\alpha^{(J)})\left\{\sqrt{1+\alpha^{(J)}J_z^2} - 1\right\}. \tag{4}$$

Relations of parameters with Watson constants and extrapolation properties of the model are discussed in [30]. The J-dependence of $\alpha^{(J)}$ in the generating function, is given by the development

$$\alpha^{(J)} = \sum_n \alpha_n \mathbf{J}^{2n}. \tag{5}$$

Linear parameters g_{nm}, u_{nm} of the Hamiltonian expansion as well as non-linear parameters of the generating functions α_n and β_n for a given vibration state have been determined in a least squares fit to experimental rotational energies. Discrepancies between observed and calculated levels given in Table 4 (the column Obs – Cal in $10^{-3}\,cm^{-1}$) and Figs. 1 and 2 (upper parts) show quite good agreement for the entire range of experimentally accessible rotational quantum numbers and also prove a consistency of our assignments. The root mean square (RMS) deviation between observed and calculated values is $0.0009\,cm^{-1}$ for 305 rotational levels of the (0 0 0) state with $J_{max} = 18$, $K_{a\,max} = 17$ and $0.0007\,cm^{-1}$ for 198 rotational levels of the (0 1 0) state with $J_{max} = 17$, $K_{a\,max} = 11$. Several outliers labeled by (e) in Table 3 (7 observed levels for (0 0 0) state and 2 observed levels for the (0 1 0) state) corresponding to blended or very weak lines were excluded from the fit because the standard deviation δ_{obs} of their determination does not provide a reliable experimental error estimation in these cases.

Values of fitted Hamiltonian parameters for (0 0 0) and (0 1 0) states with their standard errors are given in Table 4. Note that it was possible to obtain a similar RMS deviation of a fit with considerably less number of parameters. However we prefer to obtain such a set of parameters which would provide an accurate description of experimental data, and simultaneously assure physically meaningful extrapolations consistent with so called

Table 4
Fitted values of the parameters of the effective Hamiltonian for (0 0 0) and (0 1 0) states of $H_2{}^{18}O$

Parameter		(0 0 0)		(0 1 0)	
		Value	SE	Value	SE
E_{vv}				1588.27563	
α_0	$\times 10^2$	4.477767422	0.031	1.415424762	0.0011
α_1	$\times 10^4$	1.067132336	0.0079	−0.062152	
α_2	$\times 10^8$	5.287635172	0.059	9.701555245	0.13
α_3	$\times 10^{10}$	1.8235		−0.043206	
α_4	$\times 10^{15}$			2.0352	
g_{10}		11.87993852	0.0000057	11.88795872	0.000024
g_{20}	$\times 10^3$	−1.251811913	0.00014	−1.399171908	0.00081
g_{30}	$\times 10^7$	5.395683962	0.011	7.034297894	0.085
g_{40}	$\times 10^{10}$	−3.306976284	0.025	−5.231815853	0.27
g_{50}	$\times 10^{13}$	1.3445		2.6523	
g_{01}		15.651482	0.000039	18.8424396	0.00012
g_{11}	$\times 10^3$	5.718235707	0.0017	7.699877632	0.0036
g_{21}	$\times 10^6$	−1.939333991	0.019	2.322002123	0.052
g_{31}	$\times 10^9$	3.055332799	0.070	4.659577624	0.022
g_{41}	$\times 10^{12}$	0.5186		−1.7178	
g_{02}	$\times 10^1$	1.434570368	0.012	0.09866389008	0.0043
g_{12}	$\times 10^4$	4.652862021	0.035	−0.5687971522	0.0023
g_{22}	$\times 10^7$	2.356069596	0.029	1.437138832	0.050
g_{32}	$\times 10^{10}$	9.9666		−0.42314	
g_{42}	$\times 10^{13}$	−3.244		−0.44358	
g_{03}	$\times 10^4$	−5.838389273	0.053	−0.05245	
g_{13}	$\times 10^6$	−1.763410418	0.021	1.058462072	0.0058
g_{23}	$\times 10^9$	−3.266178248	0.026	1.894	
g_{33}	$\times 10^{12}$	−4.3966			
g_{04}	$\times 10^6$	−.7958849337	0.0086	−1.073564794	0.0027
g_{14}	$\times 10^9$	1.01036748	0.067	−0.009919217634	0.000036
g_{24}	$\times 10^{12}$	8.1763		−8.592232485	0.12
g_{05}	$\times 10^8$	1.085		0.89053	
g_{15}	$\times 10^{11}$	1.0223		2.7816	
g_{06}	$\times 10^{11}$	−6.0545		−2.3	
g_{07}	$\times 10^{14}$	5.328			
β_0	$\times 10^2$	4.396485501	0.11	3.749234274	0.057
β_1	$\times 10^4$	−1.244393659	0.040		
β_2	$\times 10^7$	3.185			
u_{00}		1.320951929	0.0000056	1.398496406	0.000019
u_{10}	$\times 10^4$	−5.073963802	0.0019	−5.789391333	0.0056
u_{20}	$\times 10^7$	2.690239101	0.022	3.544197177	0.056
u_{30}	$\times 10^{10}$	−1.626609466	0.10	−2.40024899	0.20
u_{40}	$\times 10^{14}$	5.692388736	1.7	9.023953334	2.1
u_{50}	$\times 10^{17}$			5.748	
u_{01}	$\times 10^3$	−1.297186101	0.0014	−3.806116496	0.0050
u_{11}	$\times 10^6$	−1.000729809	0.016	−2.324801482	0.051
u_{21}	$\times 10^9$	0.521460084	0.052	−1.759089563	0.17
u_{31}	$\times 10^{12}$	−0.047968		−4.9614	
u_{02}	$\times 10^4$	0.2521821036	0.0014	1.000485109	0.0036
u_{12}	$\times 10^7$	0.2299398745	0.0092	1.248833415	0.031
u_{22}	$\times 10^{11}$	−2.667826528	0.17	2.185222924	0.80
u_{32}	$\times 10^{13}$			1.4641	
u_{03}	$\times 10^6$	−0.213229352	0.0032	−1.636713199	0.0078
u_{13}	$\times 10^9$	0.02828419899	0.0074	−2.376925742	0.044
u_{23}	$\times 10^{13}$	3.4056			
u_{04}	$\times 10^8$	0.1297546064	0.0011	1.482109089	0.0081
u_{14}	$\times 10^{12}$	−1.0386		1.8718	
u_{05}	$\times 10^{11}$	−0.2062		−2.8332	

Note. All linear parameters g_{nm}, u_{nm} are in cm^{-1}. Non-linear parameters α_n and β_n are dimensionless.

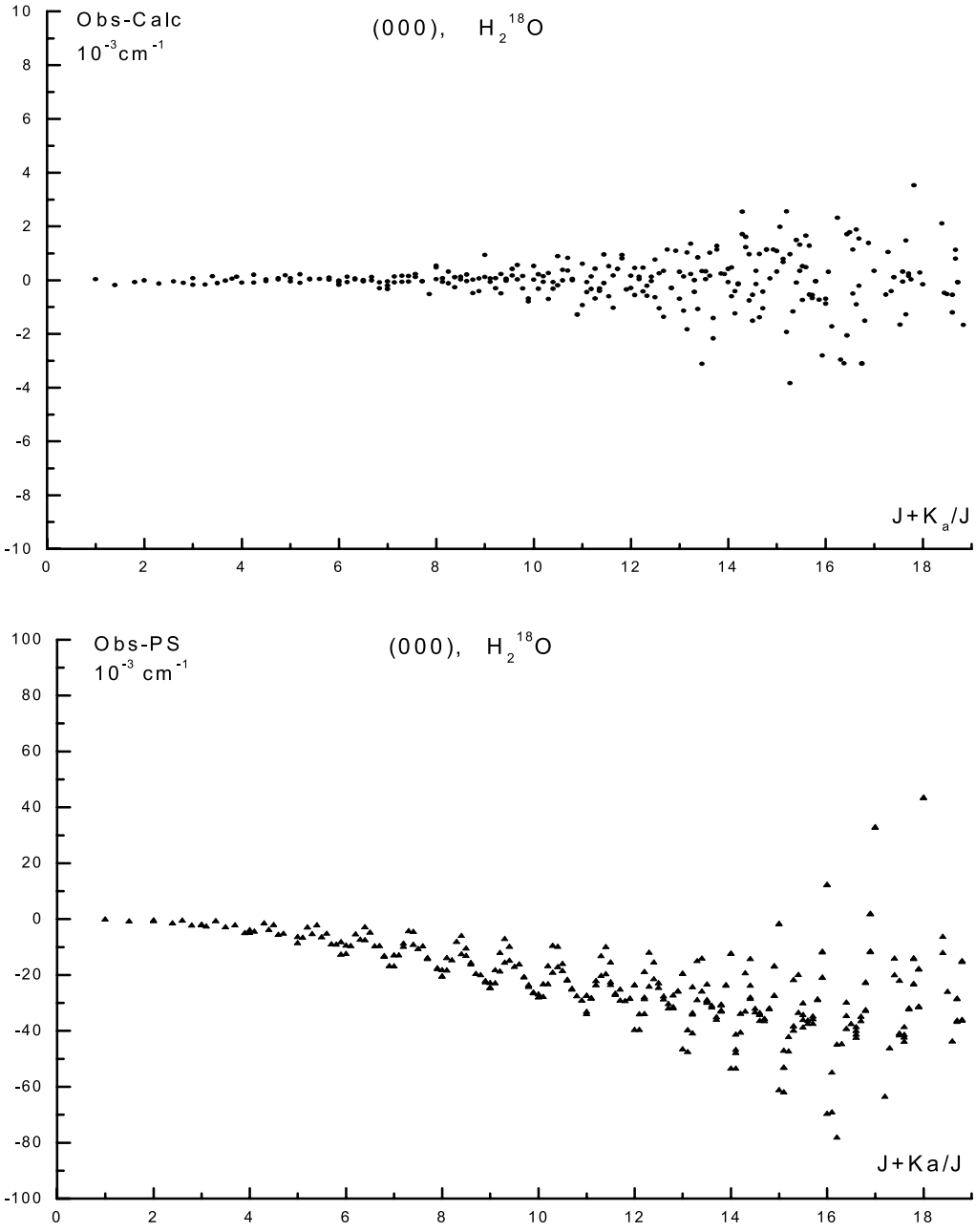

Fig. 1. Comparison of observed levels included in the fit with calculations for the (0 0 0) state of $H_2{}^{18}O$. The *upper part* corresponds to our calculations with the parameters of Table 4; the *lower part* corresponds to global PS predictions of [33]. The *abscissa* is defined as $J + (K_a/J)$ for $J > 0$ and zero for $J = 0$. Points at integer values in the horizontal axis represent J-behaviour of Obs − Calc for boundaries of a K_a manifold ($K_a = 0$ and $K_a = J$), whereas K_a-behaviour at a given J is represented by a series of points between two integer abscissa values.

"global calculations" (see the following sections for the related discussion) for a wider range of quantum numbers not yet accessible in current experimental spectra. To achieve this end we have introduced some higher order parameters whose values were constrained in a way to obtain a good agreement with global calculations outside the experimentally accessible range. These parameters correspond to the values without standard errors in Table 4.

4. Discussion: isotopic shifts and comparison with global calculations

It is instructive to compare our observations with the most accurate available global predictions from the molecular potential function by Partridge and Schwenke (PS) [33]. Discrepancies between our observed and calculated (PS) energy levels are plotted in Figs. 1b and 2b against rotational quantum numbers. The overall quali-

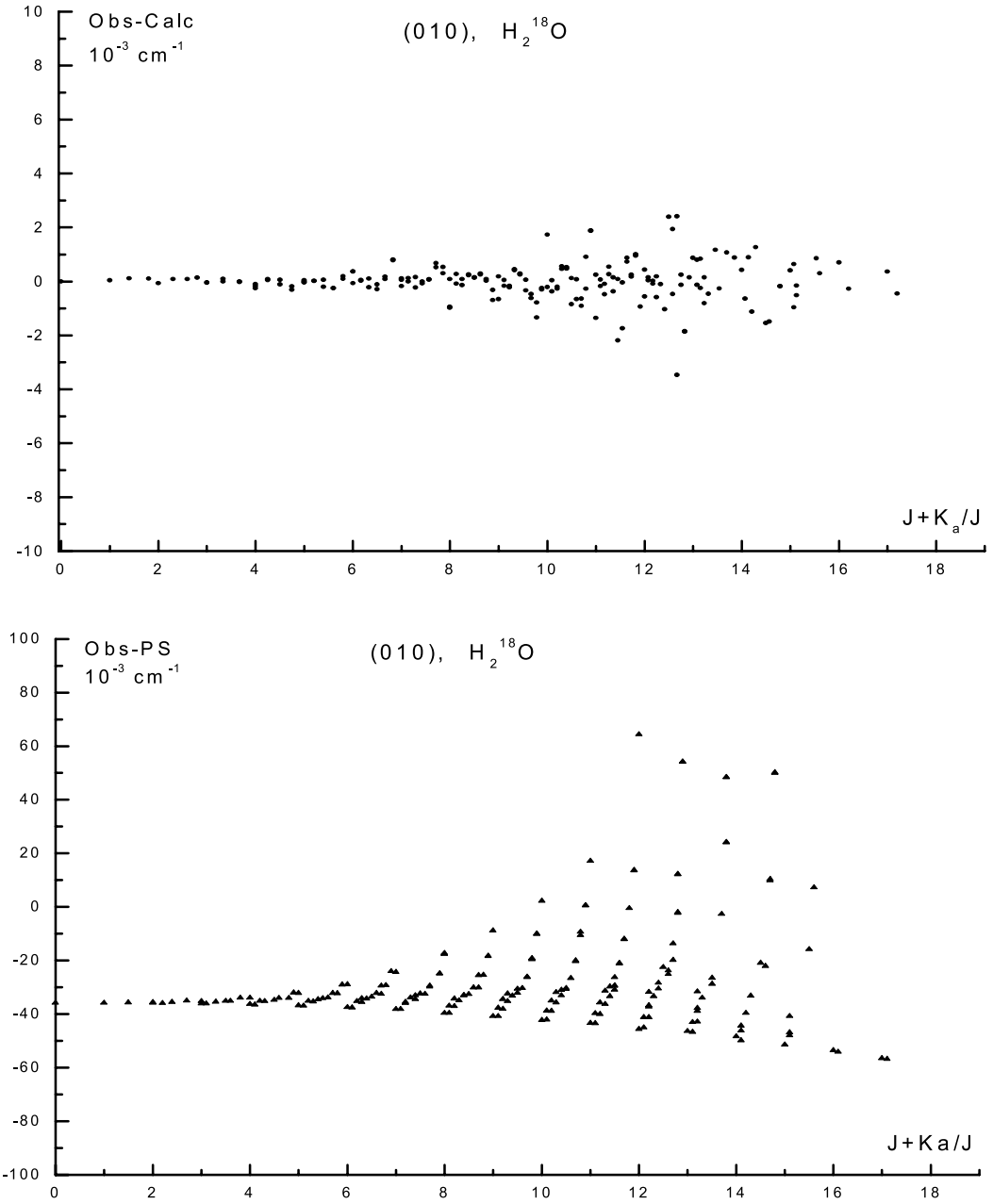

Fig. 2. Comparison of observed levels included in the fit with calculations for the (0 1 0) state of $H_2{}^{18}O$. The *upper part* corresponds to our calculations with the parameters of Table 4; the *lower part* corresponds to global PS predictions of [33]. Notations are the same as in Fig. 1.

Table 5
Summary of comparisons of calculations with observed levels and with global predictions

$H_2{}^{18}O$	(0 0 0) State	(0 1 0) State
(*A*) *Fit of observed data using the G-function model* (*parameters of Table 4*)		
J_{max}, $K_{a\,max}$	18, 17	17, 11
N_{levels} (obs)	305	198
RMS (Obs – Calc) [cm^{-1}]	0.0009	0.0007
(*B*) *Comparison of our calculations with global predictions* (*PS*) *of* [33]		
J_{max}, $K_{a\,max}$	24, 24	22, 22
$E_{rot\,max}/hc$ [cm^{-1}]	12 460	12 793
N_{levels} (calc.)	624	529
RMS (our-PS) [cm^{-1}]	0.26	0.21

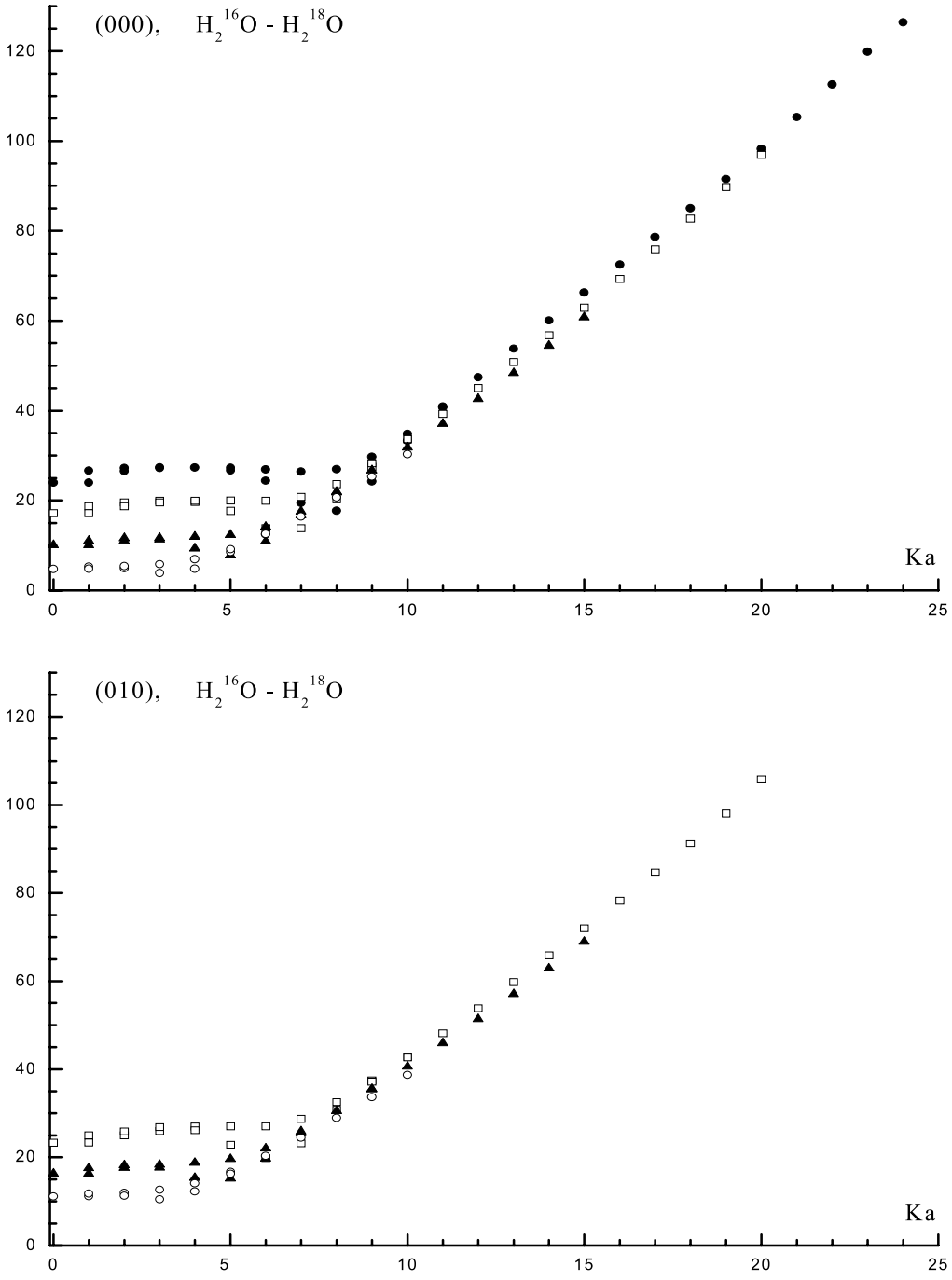

Fig. 3. Isotopic shifts [in cm^{-1}] for rotational term values versus K_a for fixed values of J for the (0 0 0) vibration state (*upper part*) and for the (0 1 0) vibration state (*lower part*). The vertical axis corresponds to $E_{J\cdot K_a} = E_{J\cdot K_a}(H_2{}^{16}O) - E_{J\cdot K_a}(H_2{}^{18}O)$. Dots correspond to series of $J = 25$, empty squares to $J = 20$, triangles to $J = 15$, and empty circles to $J = 10$.

tative agreement is surprisingly good. This gives another independent confirmation of a validity of our assignments for those levels where Table 3 shows large disagreements with previously determined energies. On the other hand this confirm remarkably good extrapolation properties of the potential function of [33]. It should be noticed that the global calculations of Partridge and Schwenke [33] are based on very careful ab initio calculations of the potential function with its subsequent optimization through a fit to spectroscopic data up to $J \leqslant 5$. Thus for $J \geqslant 6$ the comparison relies on PS predictions. Note that for the same J values the agreement in K_a behaviour is considerably better for (0 0 0) state than for the (0 1 0) state. This suggests that a further optimization of a bending section of the molecular potential function using our new data should be still possible.

Global calculations based on a full rovibrational Hamiltonian like those performed by Partridge and

Schwenke [33] have the advantage of a "birds-eye" view of the entire set of rovibrational states. Though at present for medium values of quantum numbers they are not as accurate as best "local" calculations (based on an appropriately constructed effective Hamiltonian for an isolated vibration state or for a group of closely lying vibrational states), they can give more smooth and physically consistent extrapolations for high v, J, and K_a levels.

Comparisons given in Table 5 confirm the conclusion that results from our previous analysis of $H_2{}^{16}O$ spectra that the two types of calculations, "local" and "global" once, could be used as complementary tools in spectra analysis.

Our "local" model with parameters given in Table 4 allow to achieve rather accurate data reduction (in average better than $10^{-3}\,cm^{-1}$) for presently available experimental data for (0 0 0) and (0 1 0) states as is seen in Figs. 1 and 2 (*upper parts*). On the other hand we can use global predictions to obtain parameter values giving smooth physically consistent extrapolations in a certain range of quantum numbers which is wider than that accessible experimentally. In our case the RMS deviation between our extrapolations and PS global predictions is only $0.26\,cm^{-1}$ for levels of the (0 0 0) state up to $J, K_a = 24$ and $0.21\,cm^{-1}$ for levels of the (0 1 0) state up to J, $K_a = 22$ which should correspond to a model accuracy at high-rotational energies at $E_{rot}/hc \sim 12{,}000\,cm^{-1}$. Note that such a good agreement would hardly be possible to achieve with a usual polynomial effective rotational Hamiltonian.

New experimental data and calculations allow us to study an isotopic shift of rotational levels as a function of J, K_a quantum numbers. The corresponding behaviour of shifts defined as $\Delta E_{J\cdot K_a} = E_{J\cdot K_a}\ (H_2{}^{16}O) - E_{J\cdot K_a}(H_2{}^{18}O)$ for fixed values $J = 10$, $J = 15$, $J = 20$, and $J = 24$ versus K_a in (0 0 0) and (0 1 0) vibration states is shown in Fig. 3. For those $H_2{}^{18}O$ energies which are not known experimentally the extrapolations with parameters of Table 4 are used to calculate isotopic shifts. Extensive tests of the model with available $H_2{}^{18}O$ data and comparisons with the most accurate global calculations [33] suggest that the accuracy of extrapolations for the considered states should be of the order of 0.1–$1\,cm^{-1}$ or better. Such errors are invisible on the scale of the Fig. 3. It is seen that for big K_a values the behaviour of isotopic shifts approaches a linear one in agreement with a proposal of [29]. The slopes of these asymptotics are nearly J-independent in the considered range. This can be useful for the further assignment of high K_a transitions of rare isotopic species.

Acknowledgments

S.N.M. acknowledges support from the CNRS-RFBR PICS project No. 01-05-22002. S.N.M. and Vl.G.T. thank D. Schwenke for making available his global calculations and S. Tashkun for the collaboration in RITZ project and making available the corresponding code. The authors are grateful to M.Winnewisser, B. Winnewisser, and S. Klee for the help and valuable discussions. Vl.G.T. acknowledges support from the IDRIS computer centre of CNRS.

References

[1] P.E. Fraley, K. Narahari Rao, L.H. Jones, J. Mol. Spectrosc. 29 (1969) 312–317.
[2] J.G. Williamson, K. Narahari Rao, L.H. Jones, J. Mol. Spectrosc. 40 (1971) 372–387.
[3] J.W.C. Johns, A.R.W. McKeller, Can. J. Phys. 56 (1978) 737–743.
[4] G. Guelachvili, J. Opt. Soc. Am. 73 (1983) 137–150.
[5] C. Camy-Peyret, J.M. Flaud, N. Papineau, C.R. Acad. Sci. Paris B290 (1980) 537–540.
[6] R.A. Toth, J. Opt. Soc. Am. B9 (1992) 462–482.
[7] G. Steenbeckeliers, J. Bellet, C.R. Acad. Sci. Paris B273 (1971) 471–474.
[8] F.C. De Lucia, P. Helminger, R.L. Cook, W. Gordy, Phys. Rev. A6 (1972) 1324–1326.
[9] J.W.C. Johns, J. Opt. Soc. Am. B2 (1985) 1340–1354.
[10] J. Kauppinen, E. Kyro, J. Mol. Spectrosc. 84 (1980) 405–423.
[11] R.A. Toth, J. Mol. Spectrosc. 190 (1998) 379–396.
[12] F. Matsushima, H. Nagase, T. Nakauchi, K. Takagi, J. Mol. Spectrosc. 193 (1999) 217–223.
[13] R.A. Toth, J. Margolis, J. Mol. Spectrosc. 57 (1975) 236–245.
[14] C. Camy-Peyret, J.M. Flaud, R.A. Toth, J. Mol. Spectrosc. 87 (1981) 233–241.
[15] R.A. Toth, J. Opt. Soc. Am. B10 (1993) 1526–1544.
[16] R.A. Toth, J. Mol. Spectrosc. 166 (1994) 184–203.
[17] R.A. Toth, C. Camy-Peyret, J.M. Flaud, J. Mol. Spectrosc. 67 (1977) 185–205.
[18] J.P. Chevillard, J.Y. Mandin, J.M. Flaud, C. Camy-Peyret, Can. J. Phys. 63 (1985) 1112–1127.
[19] R.A. Toth, Appl. Opt. 33 (1994) 4868–4879.
[20] J.P. Chevillard, J.Y. Mandin, J.M. Flaud, C. Camy-Peyret, Can. J. Phys. 65 (1987) 777–789.
[21] J.P. Chevillard, J.Y. Mandin, J.M. Flaud, C. Camy-Peyret, JQSRT 36 (1986) 395–399.
[22] A.S. Pine, M.J. Coulombe, C. Camy-Peyret, J.M. Flaud, J. Phys. Chem. Ref. Data 12 (1983) 413–465.
[23] J.M. Flaud, C. Camy-Peyret, J.P. Maillard, Mol. Phys. 32 (1976) 499–521.
[24] L. Wallace, P.F. Bernath, W. Livingstone, K. Hinkle, J. Busler, B. Guo, K. Zang, Science 268 (1995) 1155–1158.
[25] O.L. Polyansky, N.F. Zobov, J. Tennyson, J.A. Lotoski, P.F. Bernath, J. Mol. Spetrosc. 184 (1997) 35–50.
[26] M.P. Esplin, R.B. Wattson, M.L. Hoke, L.S. Rothman, JQSRT 60 (1998) 711–739.
[27] R. Lanquetin, L.H. Coudert, C. Camy-Peyret, J. Mol. Spectrosc. 195 (1999) 54–67.
[28] S.N. Mikhailenko, Vl.G. Tyuterev, V.I. Starikov, K.A. Albert, B.P. Winnewisser, M. Winnewisser, G. Mellau, C. Camy-Peyret, J.M. Flaud, J.W. Brault, J. Mol. Spectrosc. 213 (2002) 91–121.
[29] Vl.G. Tyuterev, J. Mol. Spectrosc. 151 (1992) 97–129.
[30] Vl.G. Tyuterev, V.I. Starikov, S.A. Tashkun, S.N. Mikhailenko, J. Mol. Spectrosc. 170 (1995) 38–58.
[31] V.I. Starikov, Vl.G. Tyuterev, Intramolecular Rovibrational Interactions and Theoretical Methods in the Spectroscopy of Non-rigid Molecules, Nauka, Moscow, 1997, pp. 1–223 [in Russian].

[32] J.K.G. Watson, J. Chem. Phys. 46 (1967) 1936–1949.
[33] H. Partridge, D.W. Schwenke, J. Chem. Phys. 106 (1997) 4618–4639.
[34] M. Birk, M. Winnewisser, E.A. Cohen, J. Mol. Spectrosc. 136 (1989) 402–445.
[35] P.S. Ormsby, K. Narahari Rao, M. Winnewisser, B.P. Winnewisser, O.V. Naumenko, A.D. Bykov, L.N. Sinitsa, J. Mol. Spectrosc. 158 (1993) 109–130.
[36] S.N. Mikhailenko, Vl.G. Tyuterev, K.A. Keppler, B.P. Winnewisser, M. Winnewisser, G. Mellau, S. Klee, K.N. Rao, J. Mol. Spectrosc. 184 (1997) 330–349.
[37] W. Quapp, M. Hirsch, G.Ch. Mellau, S. Klee, M. Winnewisser, A. Maki, J. Mol. Spectrosc. 195 (1999) 284–298.
[38] A. Maki, G.Ch. Mellau, S. Klee, M. Winnewisser, W. Quapp, J. Mol. Spectrosc. 202 (2000) 67–82.
[39] L.S. Rothman, C.P. Rinsland, A. Goldman, S.T. Massie, D.P. Edwards, J.M. Flaud, A. Perrin, C. Camy-Peyret, V. Dana, J.Y. Mandin, J. Schroeder, A. McCann, R.R. Gamache, R.B. Wattson, K. Yoshino, K.V. Chance, K.W. Jucks, L.R. Brown, V. Nemtchinov, P. Varanasi, JQSRT 60 (1998) 665–710.
[40] S.A. Tashkun, S.N. Mikhailenko, Vl.G. Tyuterev, J.L. Teffo, I. Perevalov, in preparation.